

IDEA StatiCa Member

**WP3: Comparison of the Resistance against
lateral torsional buckling of open cross-sections with
lateral and torsional restraints**

Project Partner:

IDEA StatiCa

Final Report

Report Author

ANDREAS MÜLLER M.Sc.

Responsible Investigator

Prof. Dr. techn. ANDREAS TARAS

Chair of Steel and Composite Structures

Institute of Structural Engineering (IBK)

ETH Zurich

Table of contents

1. Introduction, Objective and Scope	3
2. FE Model Description.....	5
3. General choice of global imperfections.....	7
4. Comparisons and Recommendations.....	9
4.1. Comparison of LBA Simulations	12
4.2. Comparison of the GMNIA Simulation	16
4.3. Recommendations on the calculation of lateral and torsional restraints.....	19
5. Conclusions.....	22
6. Literature and References	23

1. Introduction, Objective and Scope

The instability case of lateral torsional buckling (LTB) under bending M_y is known to be of decisive importance in the design of beams with open cross-sections (predominantly I and H sections in steel application). This instability case is characterized by a lateral displacement v and a simultaneous torsion ϑ of the member axis. The restraint of one or both of these deformation components v and ϑ represents an effective method to stabilize beams against LTB. In addition, use is made of rules to take into account the stabilizing effect of continuous and planar components directly connected to the compression chords of the beams, such as trapezoidal profiles or sandwich panels. This approach is followed, for example, in the current version of EN 1993-1-1:2010 [1], Annex BB, by specifying minimum stiffnesses for continuous lateral support S (force \times length / length) and a continuous rotational restraint C_ϑ (force \times length / length). If the corresponding values are exceeded, rigid support in the plane of lateral restraint or sufficient support against torsion can be assumed. The latter expression is to be interpreted in such a way that, if the minimum stiffness of the torsional restraint C_ϑ/k is met, no further LTB check is required. In addition, a fully provided lateral support S eliminates the lateral displacement v , yet the rotation ϑ is still active along the member and the torsional effect needs to be considered further, although the required torsional restraint to prevent LTB is minimized.

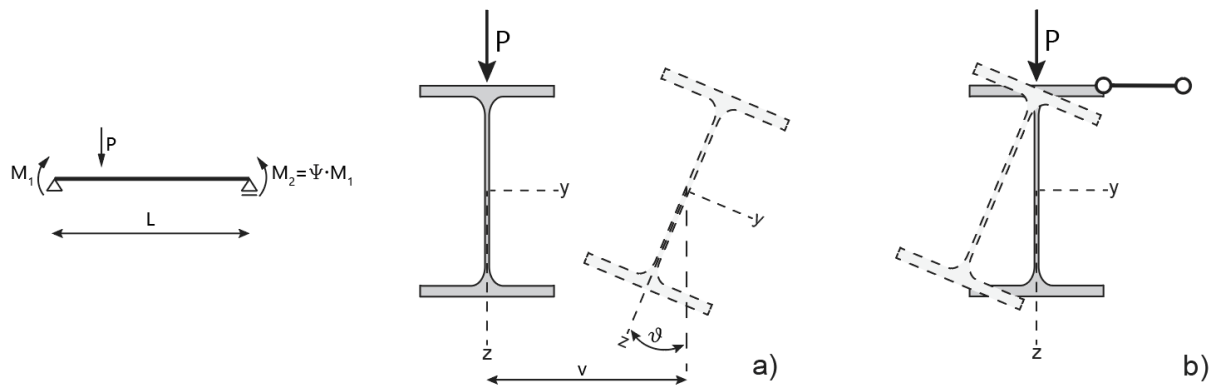


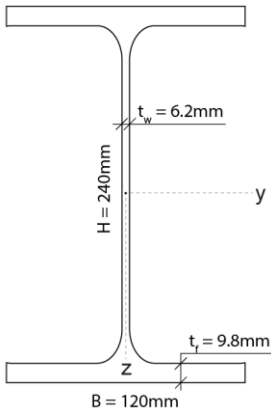
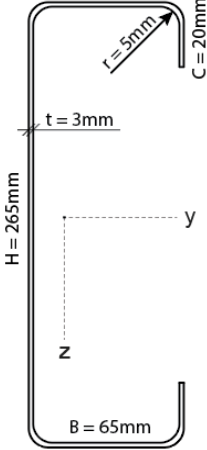
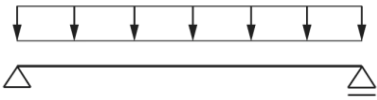
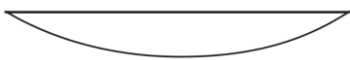
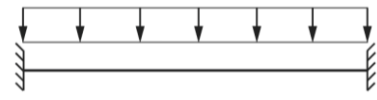





Figure 1: Representation of lateral torsional buckling for a) deformation in the case of a free axis of rotation; b) deformation in the case of a fixed axis of rotation

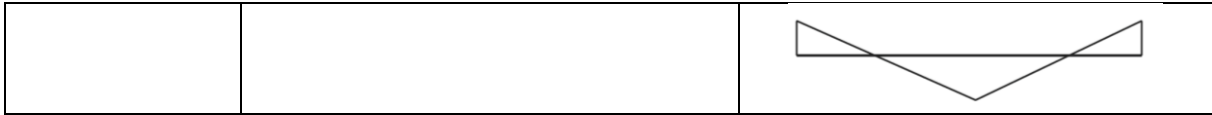
With the release of IDEA StatiCa Member application version 22.0, an additional operation is provided allowing the user to account for lateral as well as torsional restraints along the whole length or at discrete points of a member. The purpose of this report is the verification of the LBA (linear buckling analysis) and GMNIA (**g**eometrically and **m**aterial **n**onlinear **a**nalysis with **i**mperfections) simulations with lateral and torsional restraints. The resulting resistances from IDEA StatiCa Member are compared with equivalent LTBeam (LBA comparison) and Abaqus CAE 2019 [2] (LBA and GMNIA comparison) simulations. Therefore, different profiles, load situations and boundary conditions were used to evaluate the newly introduced feature to account for lateral as well as torsional restraints along the beam in a continuous manner. This offers the user a more accurate and realistic consideration of the influence of lateral torsional

buckling effects by adjacent components and thus a more economical and sustainable design of members.

For the evaluation of the bending resistances with lateral as well as torsional restraints, two different profiles were considered (IPE240 and C-shaped profile). Table 1 shows all load and boundary conditions that were taken into account throughout the study. For the IPE240 profile, cases 1 to 4 were evaluated; as for the C-shaped profile, only case 1 was considered. The steel grade was set constant to S355 throughout all investigations and considered cross-sections. In terms of the actual investigations, the rotational and lateral restraints were increased separately stepwise. In an additional step, combinations of those were selected and compared with LBA as well as GMNIA simulations from Abaqus CAE 2019 [2]. The results are presented and discussed in Sec. 4. Both, the lateral as well as the torsional restraints, were preselected to act continuously along the whole length of the beam.

Table 1: Used cross-section and considered evaluation cases

Cross-section	Properties	Cross-section	Properties
	$A = 3912 \text{ mm}^2$		$A = 1235.4 \text{ mm}^2$
	$I_y = 3.892 \cdot 10^7 \text{ mm}^4$		$I_y = 1.1945 \cdot 10^7 \text{ mm}^4$
	$I_z = 2.836 \cdot 10^6 \text{ mm}^4$		$I_z = 5.934 \cdot 10^5 \text{ mm}^4$
	$I_t = 1.288 \cdot 10^5 \text{ mm}^4$		$I_t = 3.680 \cdot 10^3 \text{ mm}^4$
	$I_w = 3.777 \cdot 10^{10} \text{ mm}^6$		$I_w = 7.90 \cdot 10^9 \text{ mm}^6$
	$W_{pl,y} = 3.66 \cdot 10^5 \text{ mm}^3$		$W_{el,y} = 89454 \text{ mm}^3$
	$L = 6000 \text{ mm}$		$L = 3000 \text{ mm}$
	Loading and support condition	Bending moment diagram	
Case 1			
Case 2			
Case 3			
Case 4			



2. FE Model Description

A general FEM-model overview of the I-shaped profile is shown in Figure 2 and Figure 3. In the case of the pinned support, Figure 2 a) shows the model boundaries simulating a fork condition. The web of the I-shaped section was connected through single-sided fillet welds to a plate so that the flanges could deform freely. The plate was additionally connected to a small horizontally applied stiffening plate, connected through a single-sided fillet weld to the related member (RM) to account for a free rotation at the boundaries. Figure 2 b) shows the boundary conditions for a fully clamped support. Butt welds were selected to achieve fixed boundary conditions of plates of I-shaped sections to the related members to avoid any failure of welds prior to failure of the sections. The setting for the generation of the mesh "Number of elements on biggest member web or flange" was adjusted from the default value of 8 to a higher value of 30 in order to match the mesh of the ABAQUS models. No other values within the "Code and calculation settings" were changed.

An equivalent Abaqus comparison model is shown in Figure 3, where the use was made of three-dimensional shell elements of type S4R. The web and the flanges were modeled with three plates intercepting in the centrelines – green dotted lines; see Figure 3 a). The fillets are not modelled explicitly but are approximated by the overlap between the web and the flanges. This approximation is well suited for rolled sections, providing a solution with safe-sided simulation results and high computational efficiency. Differences between further modelling approaches on the cross-sectional level of I-shaped profiles were already discussed and presented in [3]. For additional information, the reader is further referred to [4] and [5]. The pinned fork condition was modelled according to Figure 3 b). Kinematic couplings were used to enable opposing movements between the upper and the lower flange due to the torsional deformation caused by the out-of-plane rotation within the lateral torsional failure mode. This procedure was already successfully used in [4] and [6] and was therefore adopted within the investigations made here. The clamped boundary condition is shown in Figure 3 c). The edge nodes at both sides of the beam were connected to a reference point (RF), and placed in the profile's centre of gravity, using a multi-point tie constraint (MPC) to prevent rotations.

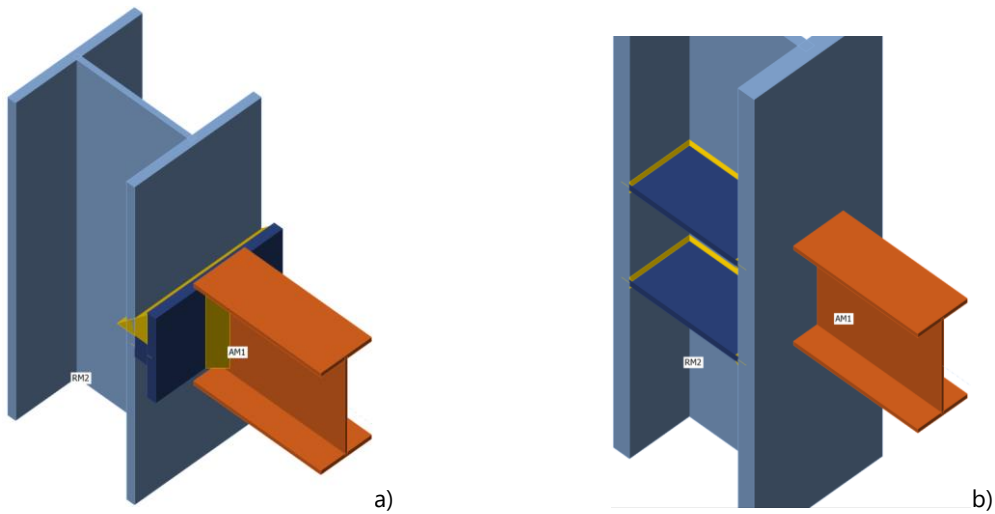


Figure 2: IDEA StatiCa Member model for a) pinned connection b) clamped connection

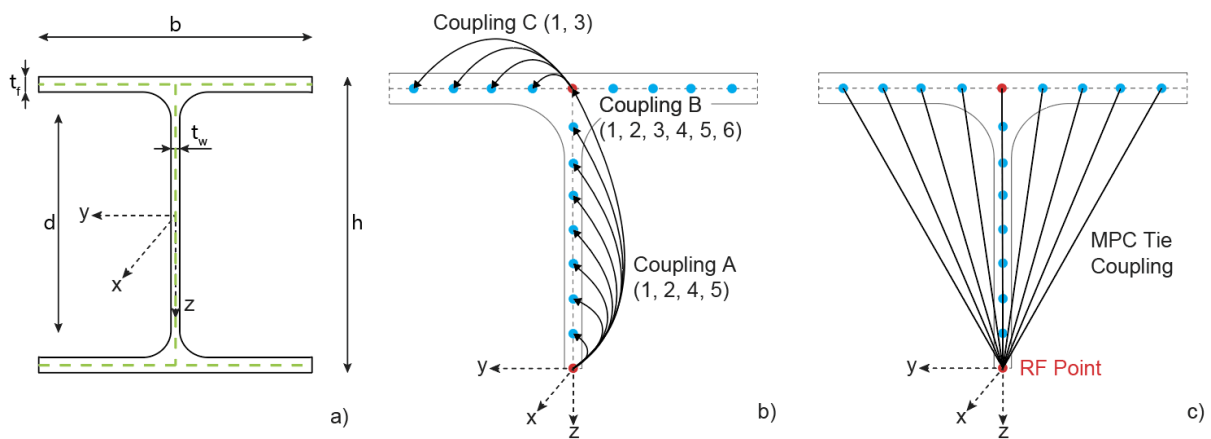


Figure 3: Abaqus model for a) pinned connection b) clamped connection

The loads were applied through concentrated forces placed directly at the nodes of the upper flange. Rotational as well as lateral restraints were modelled using spring elements attached in the middle of the upper flange (rotational restraints: Abaqus Spring1 elements; lateral restraints: Abaqus Spring2 elements).

For each model considered, a linear elastic buckling analysis (LBA) was performed in a first step, done on a geometrically perfect member without equivalent imperfections. The resulting eigenvalues and eigenmodes are used for comparison purposes between IDEA StatiCa Member, LTBeam and Abaqus. Second, the eigenshapes are used as governing imperfection shapes for the subsequent geometrically and materially nonlinear analysis with imperfections (GMNIA). The chosen material model is based on a bilinear stress-strain relation with small strain-hardening, using a reduced elastic modulus of $E/1000$. In the study presented here, steel grade S355 was used throughout all simulations and considered cross-sections.

3. General choice of global imperfections

The general preselection of the initial imperfection magnitude depends on different factors like: (i) the type of analysis according to the considered cross-section failure linked to the cross-section class, (ii) the type of imperfection considered for further calculations i.e. geometric imperfections only or equivalent imperfections including a geometric bow imperfection and additional residual stresses, (iii) the benchmark resistance in term of plastic or elastic calculation which specify the choice of imperfection. The latter corresponds to the global buckling concept of EN 1993-1-1 [1], where a cross-section dependent imperfection factor α takes both into account.

In general, two approaches have prevailed, which are treated in the literature as well as code provisions. To account for global imperfections, an eigenform affine form is obtained, usually extracted from an LBA analysis in the first step. To account for second-order effects, the used imperfection amplitude can be treated as tolerance; in many cases a value of $L/1000$ is appropriate. This assumption is combined with residual stresses, explicitly modelled along the cross-section [6]. This consideration follows the approach in [7] for the development of European buckling curves and has also been confirmed by the work in [8] and [9], as well as own investigations in [10], [11].

A more common possibility is the use of equivalent length affine imperfection amplitudes. According to the current version of EN 1993-1-1, Sec. 5.3.4(3), the equivalent imperfection amplitude for the lateral torsional buckling check (accounting for 2nd order effects) can be calculated according to Tab 5.1 [1] and Tab. 6.2 [1] for buckling around the weak axis, see Eq. (1):

$$e_{0,LT} = k \cdot j \cdot L \quad (1)$$

where:

- k is a reduction factor according to the National Annex. A value of $k = 0.5$ is recommended
- j is the design value of the imperfection amplitude ratio $e_{0,d} / L$ according to Tab. 5.1 in [1] and Table 2 of this report
- L is the member length

Table 2: Reference relative bow imperfection $j = e_{0,d} / L$ for flexural buckling

Buckling curves according to Tab. 6.2 in [1]	Elastic cross-section verification	Plastic cross-section verification
	$e_{0,d} / L$	$e_{0,d} / L$
a ₀	1/350	1/300
a	1/300	1/250
b	1/250	1/200
c	1/200	1/150

d	1/150	1/100
---	-------	-------

The selection of the lateral torsional buckling curve depends on the used formulation of the design verification, i.e. the general formulation according to EN 1993-1-1:2010, section 6.3.2.2 Tab. 6.4 or the special case in section 6.3.2.3 Tab. 6.5 for lateral torsional buckling of rolled and equivalent welded I- and H-shaped cross-sections [1]. In general, both formulations can be used in the design and verification of I-shaped members, although the general case is considered more conservative in comparison. Nevertheless, the relative reference bow imperfection $e_{0,LT}$ should be calculated from the buckling curve assigned in the general case. The chosen LTB curve may then be used to select a reference relative bow imperfection amplitude based on Table 2.

In the current draft of prEN1993-1-1:2020, 7.3.3.2 [12], a modified formulation for the determination of the length affine imperfection e_0 is presented (s. Eq. (2)).

$$e_{0,LT} = \beta_{LT} \cdot \frac{L}{\varepsilon} \quad (2)$$

where:

$\varepsilon = \sqrt{235/f_y}$ is the material parameter

β_{LT} is the reference relative bow imperfection for lateral torsional buckling according to Table 7.2 [12] and Table 3 of this report

Table 3: Reference relative bow imperfection β_{LT} for lateral torsional buckling according to prEN1993-1-1:2020 [12]

Cross-section	Condition	Elastic cross-section verification	Plastic cross-section verification
rolled	$h/b \leq 2.0$	1/250	1/200
	$h/b > 2.0$	1/200	1/150
welded	$h/b \leq 2.0$	1/200	1/150
	$h/b > 2.0$	1/150	1/100

With the introduction of a new part, the prEN1993-1-14: 2021 [14], for the design assisted by finite element analysis, an additional equation, Eq. (3), is introduced to calculate an equivalent geometric imperfection amplitude for the use in GMNIA simulations to observe LTB stability problems.

$$e_{0,LT} = \alpha_{LT} \cdot L \cdot \beta_{LT} \quad \text{but } e_{0,LT} \geq \frac{L}{1000} \quad (3)$$

where:

α_{LT} is the imperfection factor for minor axis flexural buckling, taken from EN 1993-1-1 [1], prEN1993-1-1 [12] or 1993-1-4 [13]

β_{LT} is the reference relative bow imperfection for lateral torsional buckling according to Table 5.4 [14] or Table 4 of this report, to be applied laterally to the plane of bending.

Table 4: Equivalent geometric imperfections for structural members for lateral torsional buckling [14]

Shape	β_{LT}
bow	Combination of 1/150 (half-sine wave) and 1/215 (full sine wave)
buckling shape	1/150

The imperfection factor α_{LT} depends on the lateral torsional buckling curve, which in general is chosen from the h/b profile ratio ($h/b \leq 2$ or $h/b > 2$).

The different outcomes of imperfection amplitudes between Eq. (1), (2) and (3) are represented through Fig. 4 for a $h/b \leq 2$ ratio (Figure 4 a)) and a $h/b > 2$ ratio (Figure 4 b)), respectively, for a steel grade S355 and a variety of member lengths. Using Eq. (2) from the current draft of prEN1993-1-1:2020 leads to $e_{0,LT}$ values for plastic design close to the imperfections of the current design specifications and therefore to similar capacities in the specific cases of lateral-torsional buckling. The imperfection amplitude formulation (see Eq. (3)) of the new Eurocode 3 part for the design with finite element solutions, prEN1993-1-14: 2021, on the other hand, leads to values which are always lower compared to the currently valid formulation of EN 1993-1-1:2010 represented by Eq. (1).

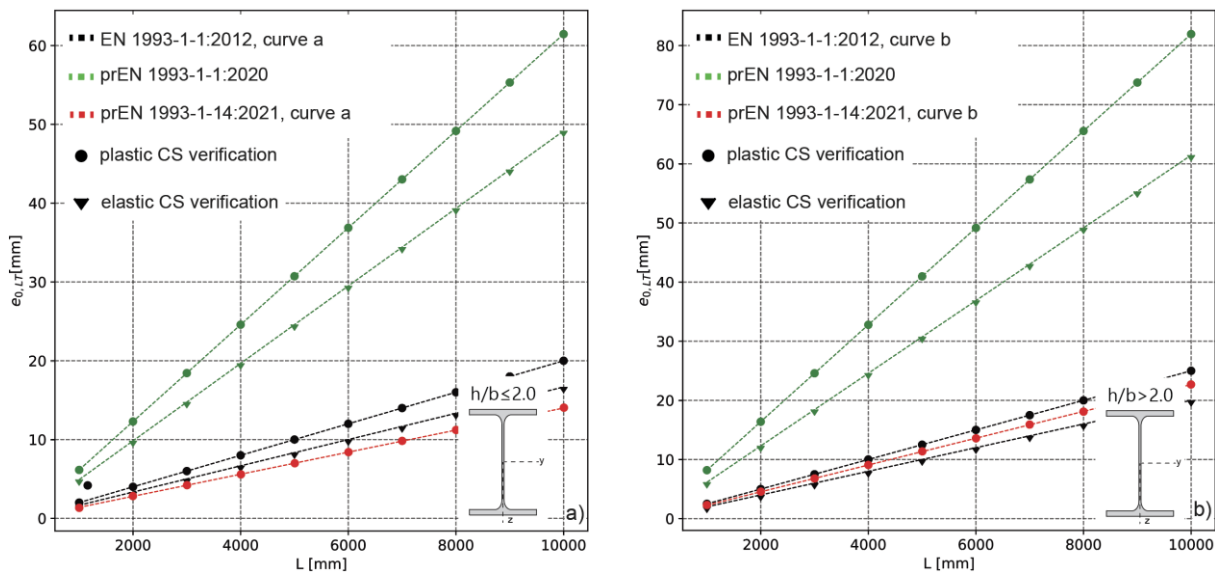


Figure 4: Imperfection amplitudes for LTB according to EN 1993-1-1:2012, prEN1993-1-1:2020 and prEN1993-1-14:2021 for the steel grade S355 a) $h/b \leq 2.0$; b) $h/b > 2.0$

4. Comparisons and Recommendations

This chapter evaluates and discusses LBA and GMNIA comparisons between IDEA StatiCa Member and Abaqus. Therefore, cases from Table 1 were used and combined with ascending values for the rotational C_θ and lateral restraint S , as well as combinations of those. LBA

simulations were performed in IDEA StatiCa Member as well as Abaqus and additionally compared with the results from the freely available software LTBeam. GMNIA results were exclusively compared between IDEA StatiCa Member and Abaqus simulations.

All results are presented in a normalized manner. For the LBA comparison (Figure 5 to Figure 7), the y-axis is described by the reached load amplification factors α_{LT} from the simulations divided by the load amplification factor from IDEA StatiCa Member without any restraints. Within the GMNIA comparison representation (Figure 8 to Figure 10), it is more feasible to use the reached maximum moment and normalize it by the plastic cross-section-dependent bending moment $M_{pl} = W_{pl,y} \cdot f_y$. Considering the cross-section modelling in IDEA StatiCa Member, the section modulus $W_{pl,y}$ was calculated without the influence of fillets.

The rotational and lateral restraints, represented along the x-axis, are normalized using the required rotational $C_{\theta,req.}$ or lateral $S_{req.}$ restraints from EN 1993-1-1:2010 [1].

The required rotational restraint $C_{\theta,req.}$ can be calculated from the following condition using Eq. (4)

$$C_{\theta} \geq \frac{M_{pl,y}^2}{EI_z} \cdot K_{\theta} \cdot K_v \quad (4)$$

where:

$M_{pl,y}$ is the plastic moment resistance about the strong axis (y-y)

EI_z is the bending stiffness about the weak axis (y-y)





K_v is 1.0 when using the plastic cross-section resistance (always the case throughout the investigations)

K_{θ} is the coefficient to take into account the LTB reduction curve, the moment distribution and the type of restraint (without or with lateral restraint).

K_{θ} can be back-calculated using Eq. (5), taking into account two additional parameters C_1 and $\lambda_{LT,req}$. The factor C_1 is a moment coefficient, which is also used for calculating the critical lateral torsional buckling moment M_{cr} . $\lambda_{LT,req}$ is the profile-dependent lateral torsional member slenderness corresponding to a buckling reduction factor χ_{LT} (EN 1993-1-1:2010, 6.3.2.3 [1]), meeting the condition where 95% of the cross-section dependent fully plastic bending moment M_{pl} (for class 1 and 2 cross-sections) is reached. All necessary values for the factor C_1 as well as the relative slenderness $\lambda_{LT,req}$ are summarized in Table 5. Coefficient K_{θ} can subsequently be calculated from Eq. (5) or directly read from Table 5 for all considered cases within this report. Table 5 was published in a similar form but for a larger variety of moment distributions in [15] and [16]. These publications are recommended for additional topic-related background information.

$$K_{\theta} = \frac{1}{\lambda_{LT,req}^4 \cdot C_1^2} \quad (5)$$

Table 5: Coefficients λ_{LT} and K_θ for different moment distributions depending on the lateral torsional buckling curves b, c, d and the type of axis of rotation. Table is based on [15].

Case	Moment distribution	C_1 k_c	Free axis of rotation			C_1 k_c	Fixed axis of rotation		
			λ_{LT} K_θ				λ_{LT} K_θ		
			b	c	d		b	c	d
1		1.12	0.584	0.532	0.486	-	0	0	0
		0.94	6.8	10.0	14.20		0	0	0
2		1.242	0.629	0.565	0.508	5.59	1.002	0.925	0.816
		0.897	4.2	6.4	9.7	0.424	0.032	0.044	0.072
3		1.35	0.667	0.594	0.528	-	0	0	0
		0.86	2.8	4.4	7.1		0	0	0
4		1.716	0.762	0.675	0.585	2.624	0.882	0.793	0.682
		0.763	1.0	1.6	2.9	0.617	0.24	0.37	0.67

The required lateral restraint $S_{req.}$ for trapezoidal sheeting is defined according to EN 1993-1-1: 2010, Annex BB.2 and expressed by Eq. (6).

$$S \geq \left(EI_w \cdot \frac{\pi^2}{L^2} + GI_t + EI_z \cdot \frac{\pi^2}{L^2} \cdot 0.25 \cdot h^2 \right) \cdot \frac{70}{h^2} \quad (6)$$

where:

- S is the shear stiffness (per unit of beam length) provided by the sheeting to the beam regarding its deformation in the plane of the sheeting to be connected to the beam at each rib.
- I_w is the warping constant
- I_t is the torsion constant
- I_z is the second moment of area of the cross-section about the weak axis
- L is the beam length
- h is the depth of the beam

In addition, also a combination of rotational and lateral restraint, continuously restrained along the beam, was evaluated and compared between the results of IDEA StatiCa Member, Abaqus and LTBeam. The normalized representation in the x-axis is chosen to be the square root of the sum between the normalized rotational restraint and the normalized lateral restraint; see Figure 7 and Figure 10. This representation was chosen solely for the purpose of comparability and is not subjected to a mechanical coupling between the effects caused by rotational and lateral restraints.

4.1. Comparison of LBA Simulations

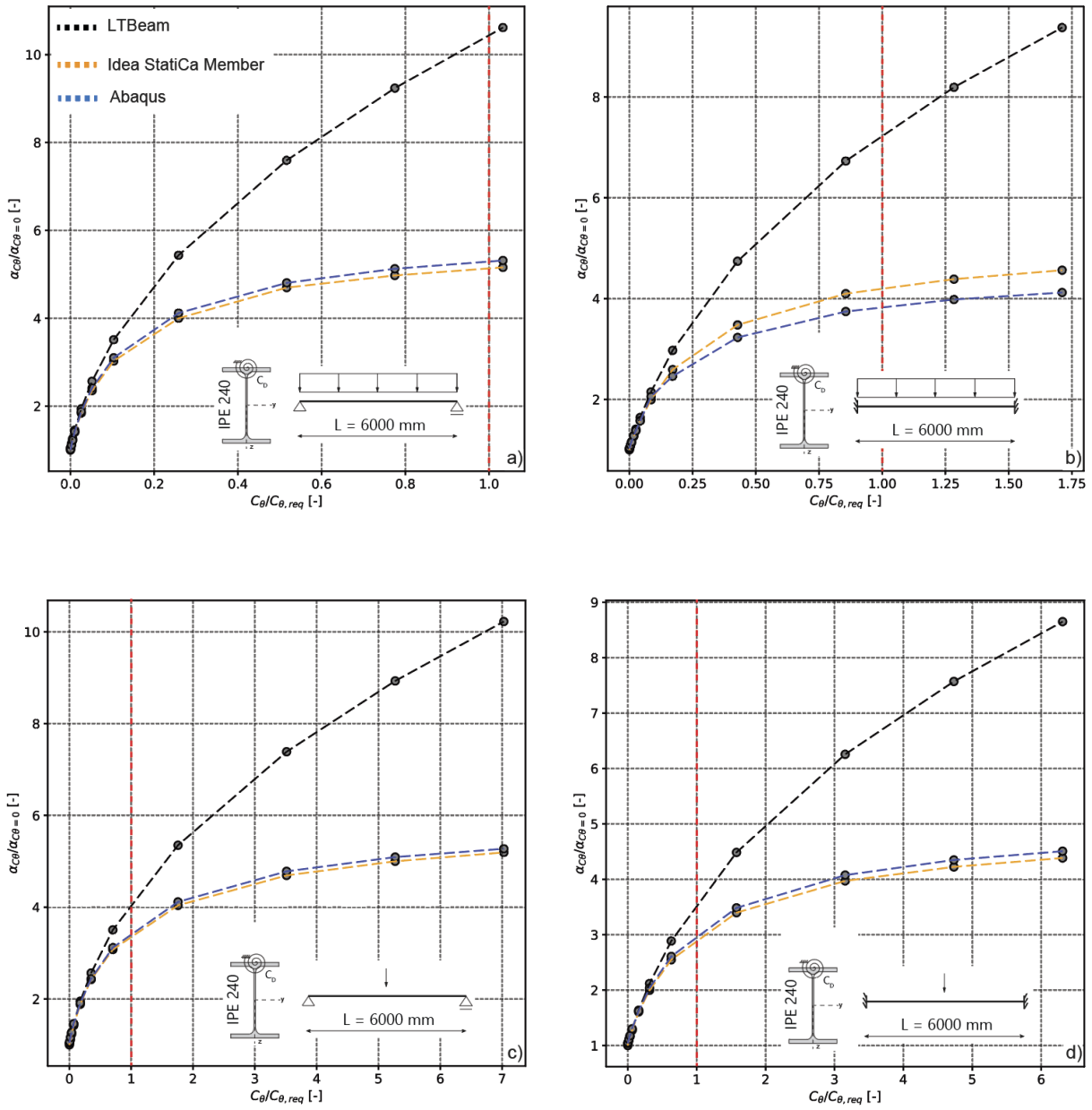


Figure 5: Comparison of LBA results for ascending values of the rotational restraint C_θ

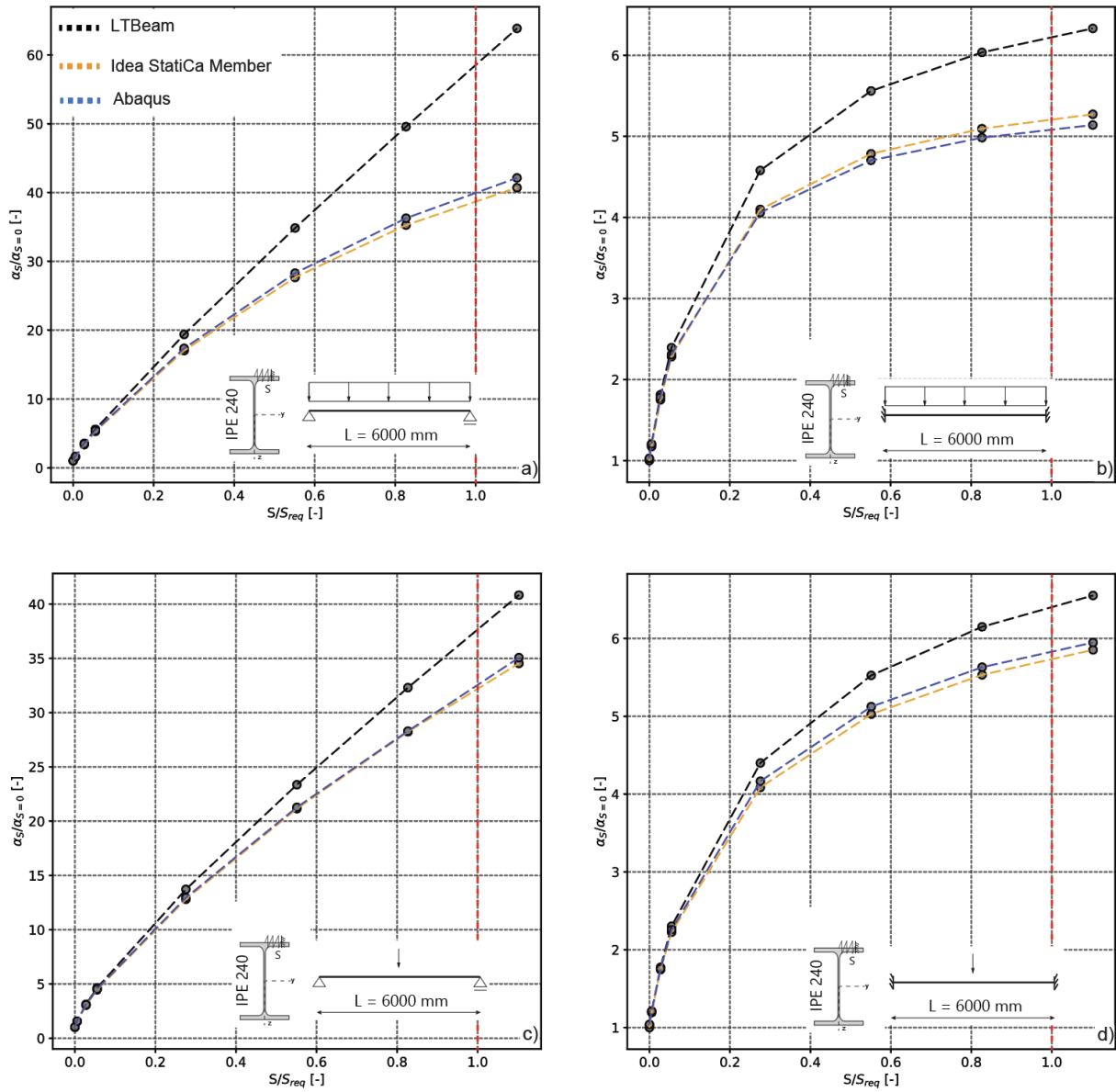


Figure 6: Comparison of LBA results for ascending values of the lateral restraint S

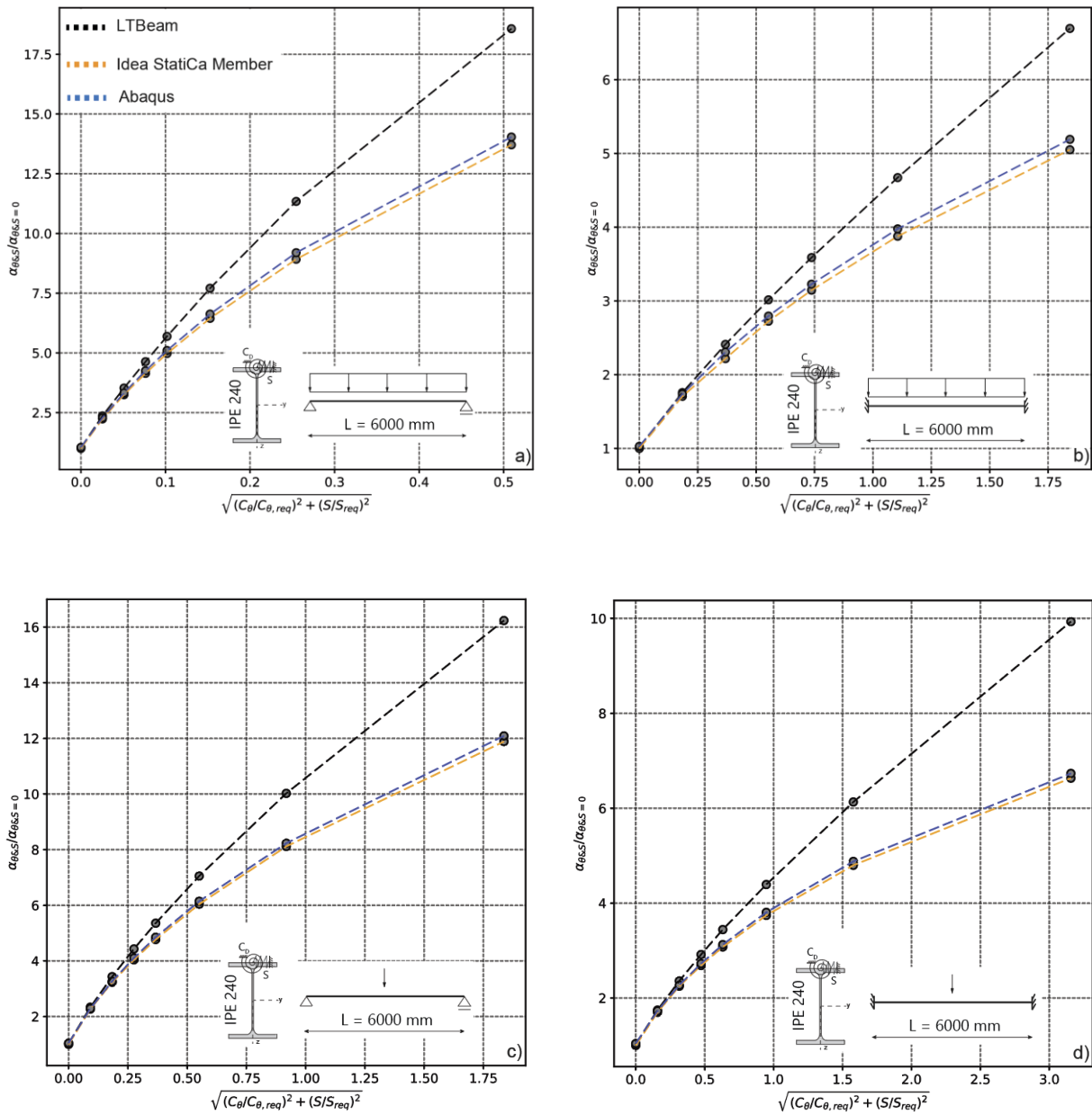


Figure 7: Comparison of LBA results for ascending values of combinations of rotational and lateral restraint

The results of the LBA comparison are summarized in Tables 5 to 7. The LBA comparison generally shows very small deviations between the results of IDEA StatiCa Member and Abaqus, for the three considered cases of ascending rotational restraints, lateral restraints and a combination of those two, related to the different cases from Table 1. A maximum difference of 7% (s. Figure 5 b)) is identified for case 2 (clamped boundary condition with line load) and rotational support C_{θ} . This can be attributed to small differences within modelling approaches of the boundary conditions between IDEA StatiCa Member and Abaqus. However, all other results show significantly smaller differences between the bifurcation loads and are therefore well within the range of acceptance. It should be noted here that IDEA StatiCa Member provides in

the most cases a slightly lower linear buckling factor than Abaqus. Comparing the results from the simulations in IDEA StatiCa Member and Abaqus with the results from LTBeam leads to significantly higher differences in the achieved theoretical linear elastic load amplification factor. The results by LTBeam constantly increase with ascending rotational or lateral restraints, without reaching a physically meaningful plateau value, compared to the results of IDEA StatiCa Member or Abaqus. This is due to the fact that LTBeam uses only member elements that cannot account for section deformation and therefore overestimate the critical buckling load.

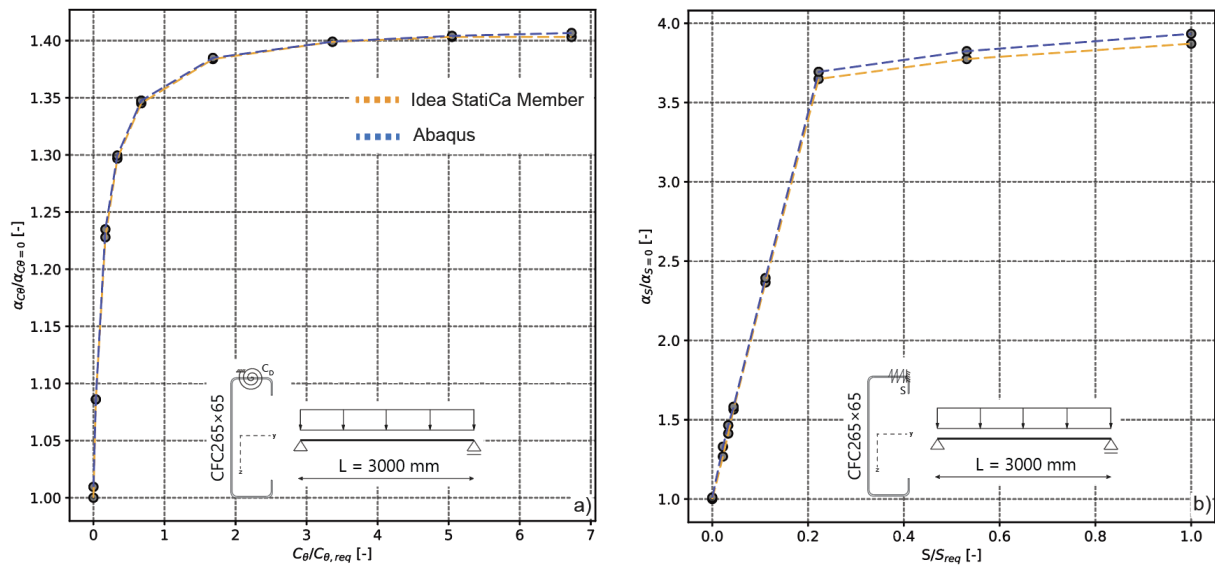


Figure 8: Comparison of LBA results for: a) ascending values of the rotational restraint C_θ ; b) ascending values of the lateral restraint S

The comparison of the C-shaped section is shown in Figure 8. The achieved critical elastic buckling factors calculated in IDEA StatiCa are always lower compared to Abaqus. The deviations lie within an acceptable range between 2% to 3%.

4.2. Comparison of the GMNIA Simulation

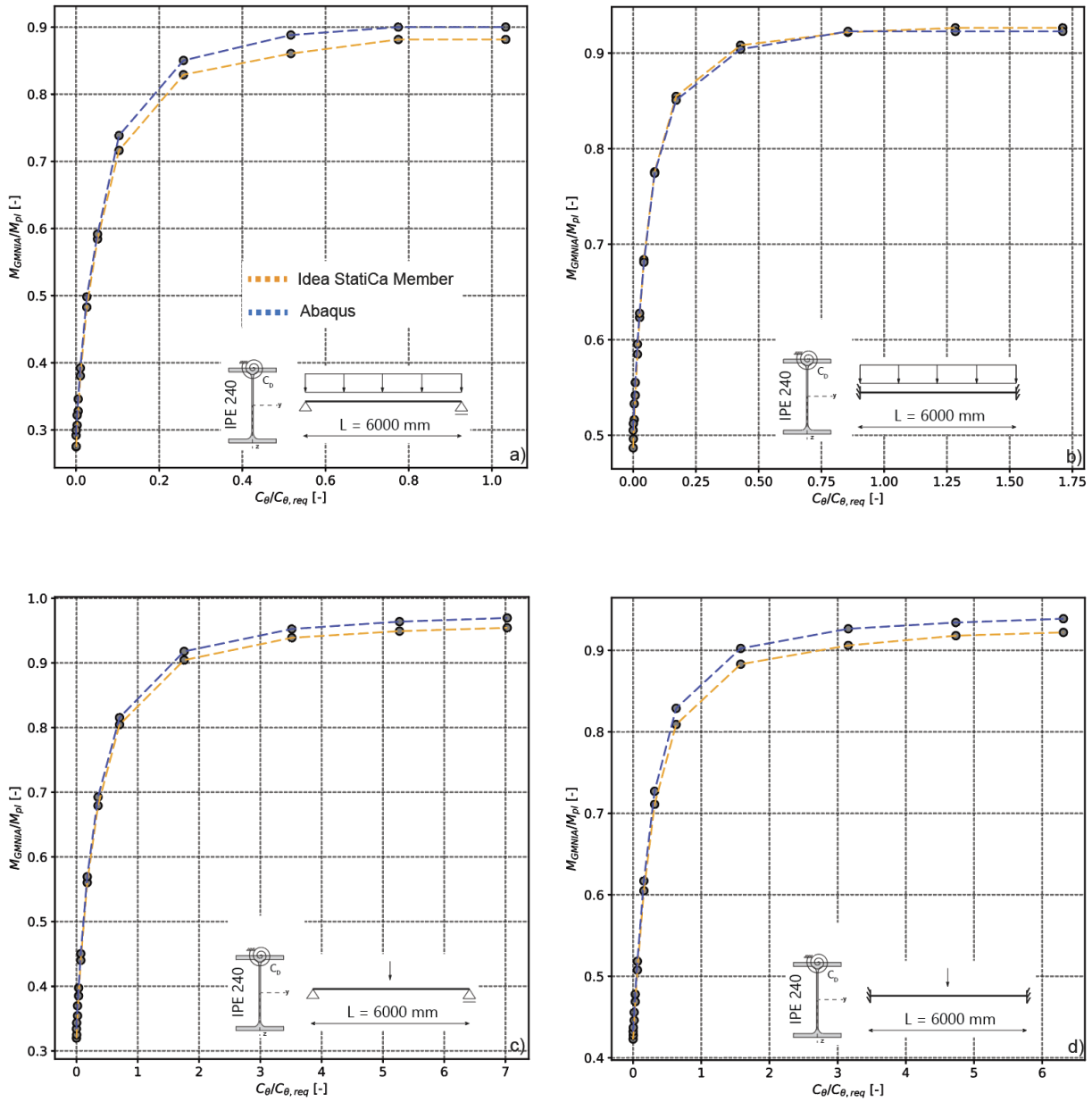


Figure 9: Comparison of GMNIA results for ascending values of the rotational restraint C_θ

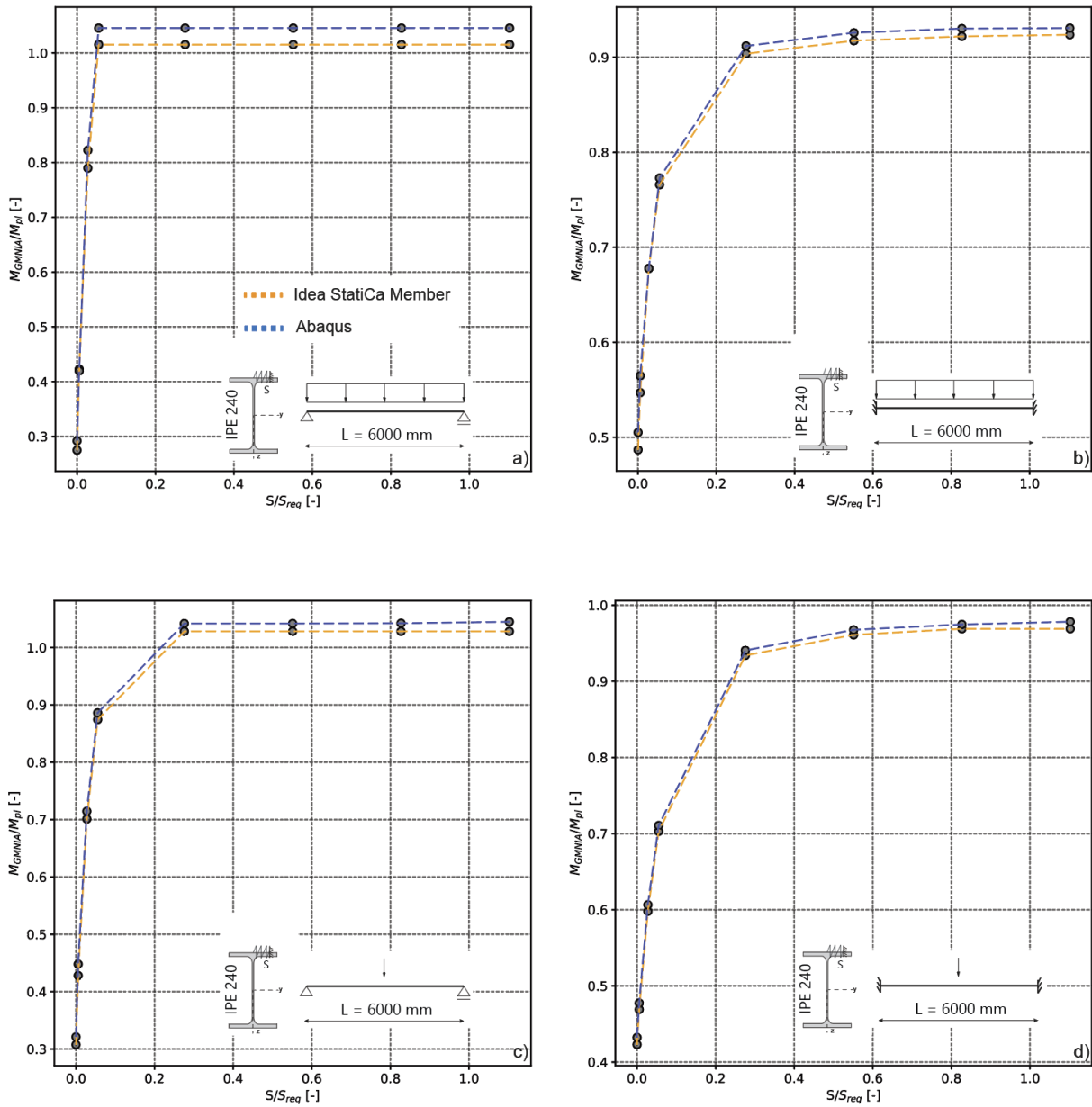


Figure 10: Comparison of GMNIA results for ascending values of the lateral restraint S

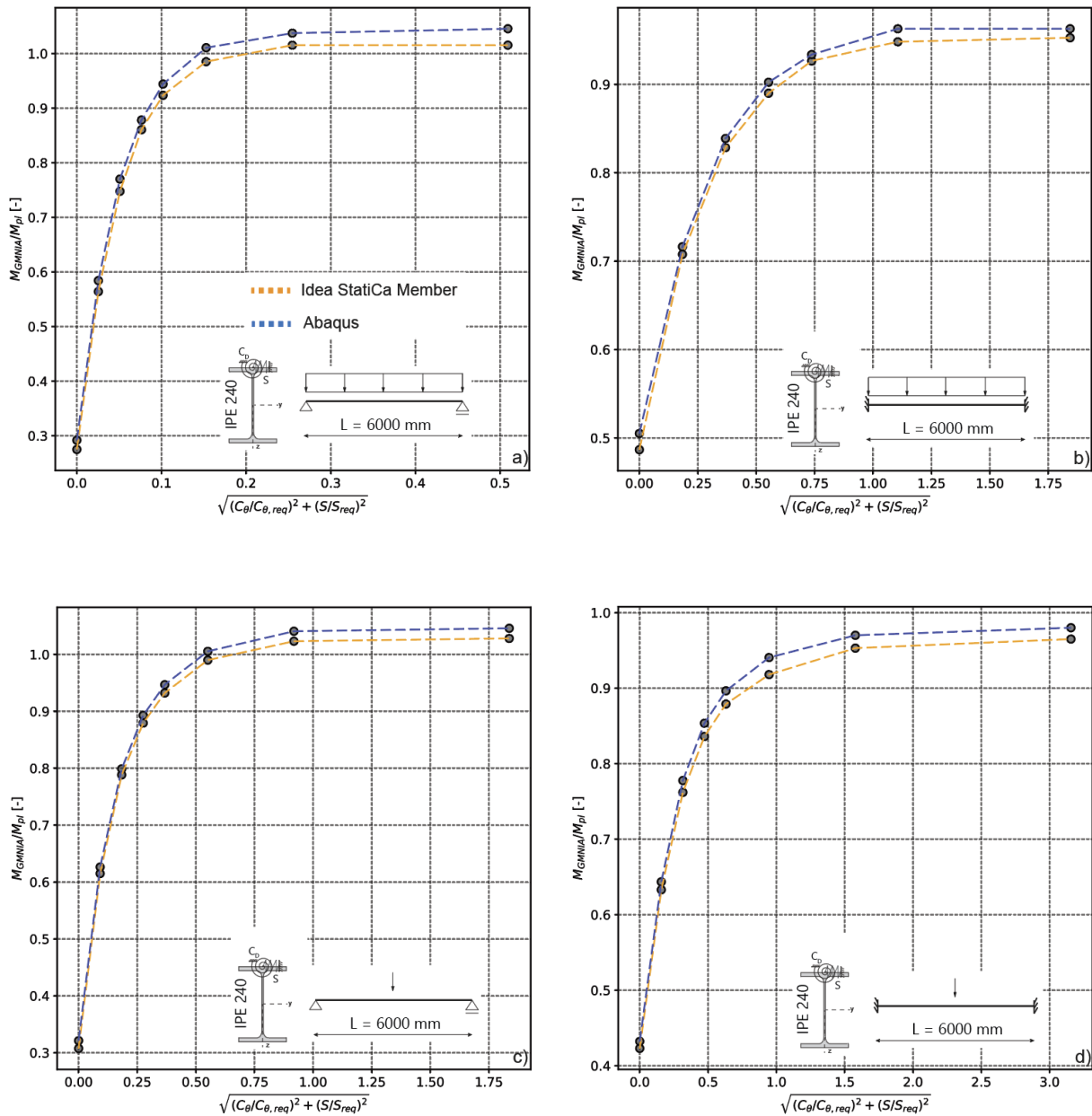


Figure 11: Comparison of GMNIA results for ascending values of combinations of rotational and lateral restraint

The GMNIA results are summarized in Figure 9 to Figure 11, again for the load conditions displayed in Table 1. The chosen imperfection amplitude throughout all calculations was set to the length dependent ratio of $L/1000$ [17], since the general goal was a direct comparison between resistances from rising torsional or lateral restraints and not investigations on the impact of different imperfection amplitude formulations. The resistance comparison between IDEA StatiCa Member and Abaqus generally shows only minor deviations of the achieved maximum moments being no greater than 4 %. The basic requirement that approximately 95% of the plastic load-bearing capacity should be reached by using the limit values for the rotational restraint C_{θ} – all necessary values are summarized within Table 5 of this report – can be confirmed in most cases. It should be noted that the K_{θ} are more or less exact approximations to

fulfill the “95% rule” and that there is no exact consistency with the LTB curves. Since the selected I-shaped profile lies exactly on the boundary between buckling curves b and c (according to the current EN 1993-1-1), and these in turn try to describe a large number of profiles being both optimistic and conservative, it is not always possible to meet the limit values exactly. The achieved loads calculated by IDEA StatiCa Member are always slightly lower than the calculated loads in Abaqus. Again, this level of deviation is common and well within the range of acceptability.

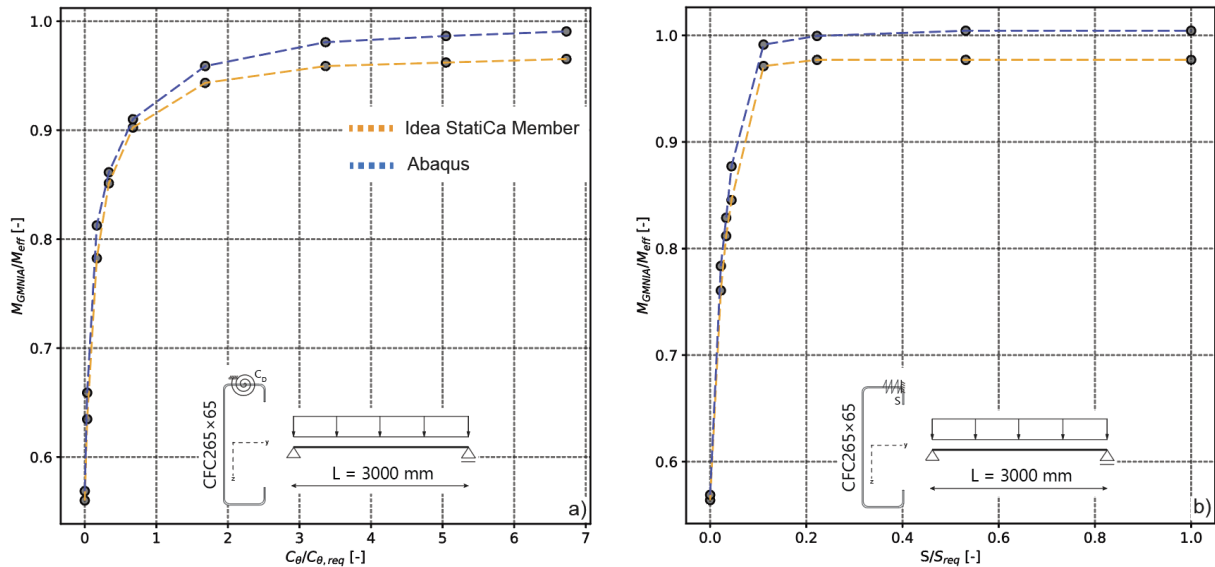


Figure 12: Comparison of GMNIA results for: a) ascending values of the rotational restraint C_θ ; b) ascending values of the lateral restraint S

The GMNIA comparison for the C-shaped profile is shown in Figure 12 for ascending values of the torsional as well as the lateral restraint. The y-axis describes the acquired maximum reached moments within the simulations, normalized by the effective moment $M_{eff} = f_y \cdot W_{eff}$. This representation makes more sense, since the used profile is attributed to cross-section class 4, failing to reach the yield strength due to local elastic buckling. Nevertheless, the achieved loads, calculated by IDEA StatiCa Member are always slightly lower than the calculated loads in Abaqus. Again, this level of deviation (approximately up to 5%) is common and well within the range of acceptability.

4.3. Recommendations on the calculation of torsional and lateral restraints

Following recommendations on the calculation of the torsional as well as the lateral restraints are limited to corrugated panels and sandwich panels.

4.3.1. Determination of rotational restraint

In general, the existing rotational restraint can be regarded as a system of several springs connected in series [18], [19].

$$available\ C_g = \frac{1}{\frac{1}{C_{gM}} + \frac{1}{C_{gA}} + \frac{1}{C_{gP}}} \quad (7)$$

where:

C_{gM} [kNm / m] is the theoretical rotational restraint from the bending stiffness of the supporting component

C_{gA} [kNm / m] is the rotational restraint from the deformation of the connection

C_{gP} [kNm / m] is the rotational restraint from the profile deformation

The available rotational restraint C_{gM} from the bending stiffness of the supporting components is determined for a one field girder through the derivation in Eq.(8) as well as Figure 13.

$$\begin{aligned} \varphi &= \frac{1}{2} \cdot 1 \cdot M \cdot \frac{a}{EI_a} = 1 \\ C_{gM} &= \frac{M}{\varphi} \\ C_{gM} &= \frac{2 \cdot EI_a}{a} = \frac{k \cdot EI_a}{a} \end{aligned} \quad (8)$$

where:

EI_a is the bending stiffness of the supporting components

k is a system dependent factor: $k = 2$ for a simply supported one and two field girder;
 $k = 4$ for continuous beam with three or more fields and equivalent spans

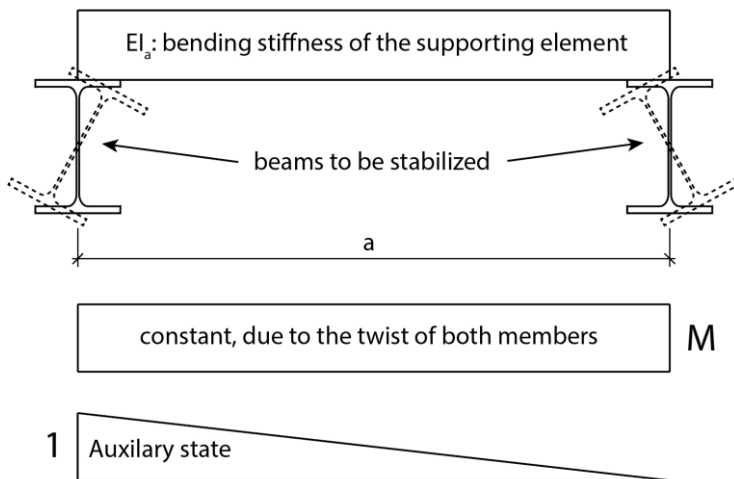


Figure 13: Available rotational restraint C_{gM} from bending stiffness of supporting elements

The rotational restraint C_{gP} from profile deformation depends on how the moment is transmitted between the beam to be stabilized and the adjacent component. If the surface contact

interaction and the transfer through torsional moments in the chord are not taken into account, the following equation applies in general [19], [20]:

$$C_{gp} = \frac{E}{4 \cdot (1 - \nu^2)} \cdot \frac{1}{\frac{h}{s^3} + c_1 \cdot \frac{b}{t^3}} \quad (9)$$

where:

b, t is the width or thickness of the top flange of the supported beam in [cm]

s is the thickness of the web of the supported beam in [cm]

h is the distance between the flange center lines of the supported beam in [cm]

ν is the Poisson's ratio of steel. For the simplification within Eq.(10) and Eq.(11) a Poisson's ratio of $\nu = 0.3$ was used.

c_1 is a profile and load dependent factor [20]:

- for I-shaped profiles loaded by normal pressure or suction pressure: $c_1 = 0.5$
- for C-shaped profiles or similar loaded by normal pressure: $c_1 = 0.5$
- for C-shaped profiles or similar loaded by suction: $c_1 = 2.0$

Therefore, the general form of Eq.(9) can be further simplified and written as follows. Eq.(10) can be used approximately for common steel beams loaded by normal pressure and Eq.(11) for C-shaped profiles loaded by suction pressure:

$$C_{gp} \approx 5000 \cdot \frac{s^3}{h} \quad (10)$$

$$C_{gp} \approx 2500 \cdot \frac{s^3}{h} \quad (11)$$

The rotational restraint c_{gA} from the deformation of the connection can be determined according to Eq.(12). This formulation was originally introduced in [21] and further adopted by the Technical Working Group TWG 7.9 for sandwich panels and related structures in [16].

$$C_{gA} = \frac{3}{2} \cdot \frac{c_{g1}}{\left(\frac{c_{g1}}{c_{g1} + c_{g2}} + 1 \right)} \quad (12)$$

All additional information, recommendations on individual parameters as well as worked out examples on the determination of c_{gA} shall be taken from [16].

4.3.2. Determination of lateral restraint

The shear stiffness for trapezoidal plates can be determined according to EN 1993-1-3 [22] as follows:

$$S = 1000 \cdot \sqrt{t^3} \cdot \left(50 + 10 \cdot \sqrt[3]{b_{roof}} \right) \cdot \frac{s}{h_w} \quad (13)$$

where:

- t is the thickness of the trapezoidal sheet in [mm]
- b_{roof} is the width of the roof in [mm] (for a gable roof the distance from the eaves to the apex)
- s is the distance between the beams in [mm]
- h_w is the height of the trapezoidal sheet wave in [mm]

The shear stiffness for sandwich panels according to EN 1993-1-3 [22] is determined by Eq.(14).

$$S = \frac{k_v}{2B} \sum_{k=1}^{n_k} c_k^2 \quad (14)$$

where:

- k_v is the stiffness of the connecting elements
- B is the width of the sandwich panel
- n_k is the number of pairs of connecting elements
- c_k is the distance between pairs of connecting elements

5. Conclusions

The instability case of lateral torsional buckling is a common problem in structures with wide span roofs, crane runway girders subjected to high loads or thin-walled cold-formed or stainless steel systems. The stabilizing effect of adjacent members and roof coverings has been known for a long time, resulting in implementations throughout code provision. In practical applications, however, these specifications are not always easy to implement, therefore often neglected, leading to a high level of conservatism and unnecessarily higher material consumption.

The newly introduced feature in IDEA StatiCa Member application version 22.0 allows accounting for lateral as well as torsional restraints along the whole length or at discrete points of a member. This design-by-analysis approach was verified in this report for various load scenarios, boundary conditions and profiles. The comparison between the calculations in the IDEA StatiCa Member software and the FEM program Abaqus showed generally small deviations in the LBA

as well as GMNIA results with a maximum difference of 5% in individual cases. This level of deviation is common and well within the range of acceptability.

Additionally, Sec. 3 provides information on the choice of imperfection amplitudes, based on different code provisions i.e. EN 1993-1-1, prEN1993-1-1 and prEN1993-1-14. Sec. 4.3 gives the user an overview and recommendations on the determination of values for the torsional and lateral restraints for corrugated panels and sandwich panels.

6. Literature and References

- [1] EN 1993-1-1 (2010) Eurocode 3. Design of steel structures – Part 1-1: General rules and rules for buildings. CEN – European Committee for Standardization. Brussels.
- [2] Abaqus. Reference manual (2016), version 6.16. Simulia, Dassault Systèmes, France.
- [3] Taras, A.; Müller, A. (2021) IDEA StatiCa Member, WP1-2: Comparison of the Buckling Resistance of I-shaped cross-sections. Chair of Steel and Composite Structures, ETH Zurich. Available at: <https://www.ideastatica.com/support-center/comparison-of-buckling-resistance-of-i-shaped-cross-sections>
- [4] Taras, A. (2011) Contribution to the Development of Consistent Stability Design Rules for Steel Members. Dissertation, Institut für Stahlbau und Flächentragwerke, TU Graz, Heft 16, Graz.
- [5] Kindmann, R.; Kraus, M. (2019) FE-Berechnung mit Fließzonen für Tragfähigkeitsnachweise nach DIN EN 1993-1-1, Vereinfachte Berechnungsmethode für stabilitätsgefährdete Bauteile. Stahlbau 88, H. 4, S. 354-362.
- [6] Müller, A.; Taras, A. (2021) Kippstabilität von Trägern mit Drehbettung – Einfluss und Anwendung der neuen Regelungen in prEN1993-1-1:2020. Stahlbau 90, H. 9, S. 636-652.
- [7] Beer, H.; Schulz, G. (1970) Bases Théoriques des Courbes Européennes de Flambement. Constr. Métallique, Vol. 3, pp. 37-57.
- [8] Taras A., Greiner R. (2010), New design curves for lateral torsional buckling – Proposal based on a consistent derivation, Journal of Constructional Steel Research, 70, Elsevier London/Amsterdam, <https://doi.org/10.1016/j.jcsr.2010.01.011>
- [9] Greiner, R., Taras, A., New design rules for LT and TF buckling with consistent derivation and code-conform formulation, Steel Construction - Design and Research 3/2010, pp. 176-186, Wiley VCH- Ernst & Sohn, New York/Berlin, <https://doi.org/10.1002/stco.201010025>
- [10] Toffolon A.; Müller A.; Taras A. (2019) Experimental and numerical analysis of the local and interactive buckling behaviour of hollow sections. Conference Paper, Nordic Steel Conference 2019
- [11] Toffolon A.; Meng X.; Taras A.; Gardner L. (2019) The generalised slenderness-based resistance method for the design of SHS and RHS. Steel Construction, Vol. 12, Issue 4, Wiley.
- [12] prEN 1993-1-1 (2020) Eurocode 3: Design of steel structures – Part 1-1: General rules and rules for buildings. CEN – European Committee for Standardization. Brussels.

- [13] EN 1993-1-4 (2015) Eurocode3: Design of steel structures – Part 1-4: General rules – Supplementary rules for stainless steel CEN – European Committee for Standardization. Brussels.
- [14] prEN 1993-1-14 (2021), Eurocode 3: Design of steel structures – Part 1-14: Design assisted by finite element analysis, CEN/TC 250/SC 3 N 3437, Comité Européenne de la Normalisation (CEN), Brüssel, 2021.
- [15] Lindner, J. (2008) Zur Aussteifung von Biegeträgern durch Drehbettung und Schubsteifigkeit. Stahlbau 77, H. 6, S427-435.
- [16] ECCS TC7 – Technical Working Group TWG 7.9 Sandwich Panels and Related Structures, European Recommendations on the Stabilization of Steel Structures by Sandwich Panels, CIB Publication 379, ISBN 978-90-6363-081-2.
- [17] DIN EN 1090-2 (2018) Execution of steel structures and aluminium structures – Part 2: Technical requirements for steel structures. CEN – European Committee for Standardization. Brussels.
- [18] Lindner, J., Kurth, W. (1980) Drehbettungsbeiwerte bei Unterwind. Bauingenieur 55, S. 365-369.
- [19] Lindner, J. (1987) Stabilisierung von Trägern durch Trapezbleche, Stahlbau 56, S. 9-15.
- [20] Lindner, J. (1987) Stabilisierung von Biegeträgern durch Drehbettung – eine Klarstellung. Stahlbau 56, S. 365-373.
- [21] Dürr, M. (2008) Die Stabilisierung biegedrillknickgefährdeter Träger durch Sandwichelemente und Trapezbleche (Stabilization of beams prone to lateral torsional buckling by sandwich panels and trapezoidal sheeting). Karlsruhe: Berichte der Versuchsanstalt für Stahl, Holz und Steine der Universität Fridericiana in Karlsruhe, 5. Folge Heft 17 (<http://digbib.ubka.uni-karlsruhe.de/volltexte/documents/148221>).
- [22] EN 1993-1-3 (2006) Eurocode 3: Design of steel structures – Part 1-3: General rules – Supplementary rules for cold-formed members and sheeting. CEN - European Committee for Standardization. Brussels.